Slattery, J. C., "Interfacial Effects in the Entrapment and Displacement of Residual Oil," *AIChE J.*, **20**, 1145 (1974).
Stegemeier, G. L., "Mechanisms of Entrapment and Mobilization of Oil in Porous Media," AIChE 81st Nat. Meeting, Kansas City, Mo. (Apr. 1976).
Tien, Chi and A. C. Payatakes, "Advances in Deep Bed Filtration, *AIChE J.*, **25**, 737 (1979).
van Brakel, J., "Pore Space Models for Transport Phenomena in Porous Media. Review and Evaluation with Special Emphasis on Capillary Liquid Transport," *Powder Technol.*, **11**, 205 (1975).
Wasan, D. T., K. Sampath, J. J. McNamara, et al., "The Mechanism of Oil Bank Formation, Coalescence in Porous Media and Emulsion Stability," *Proc. 4th DOE Symposium on Enhanced Oil and Gas Recovery*, Tulsa, Okla. (Aug. 29-31, 1978).
Wasan, D. T., J. J. McNamara, S. M. Shah, et al., "The Role of Coalescence Phenomena and Interfacial Rheological Properties in Enhanced Oil Recovery: An Overview," *J. of Rheology* **23**, No. 2, 181 (1979).

Manuscript received January 17, 1979; revision received October 4, and accepted October 11, 1979.

Dendritic Deposition of Aerosols by Convective Brownian Diffusion for Small, Intermediate and High Particle Knudsen Numbers

A. C. PAYATAKES
and
L. GRADOŃ
Chemical Engineering Department
University of Houston
Houston, Texas 77004

When an aerocolloidal suspension flows through a fibrous filter, particles deposit on the fibers and form dendrites. Similar phenomena are observed with collectors other than fibers, provided that the characteristic dimension of the collector does not exceed that of the particles by more than one to two orders of magnitude. This deposition pattern leads to marked increases in capture efficiency and pressure drop, as particles accumulate within the filter. In previous publications, theoretical models of this process were developed for the cases of deposition by interception alone and of deposition by combined inertial impaction and interception. Consequently, those works apply to aerosol particles with diameters of 1 μm or larger. Here we extend the model to the case of submicron particles, where the main transport mechanism is Brownian diffusion. To keep things specific, we consider fine fibers as collectors, but the model can be easily converted to other geometries. We present solutions for the cases of nonslip flow around the fiber and nonslip, slip and free molecular flow around particles. Unlike deposition by inertial impaction and/or interception, convective Brownian diffusion forms dendrites over the entire fiber surface.

SCOPE

Aerosol filtration in fibrous mats is one of the most efficient methods of solid-gas separation, especially in the case of submicron particles. Fibrous filters are compact, provide excellent capture efficiency and present minimal resistance to flow. For given pressure drop, the flow rate through a fibrous filter is several times higher than that through a fabric filter of equal area, without sacrifice in capture efficiency or danger of blinding. Their main drawback seems to be that in situ cleaning is usually difficult. Hence, most industrial applications are still confined to cases where high efficiency is demanded and where the use of disposable filter elements is practical (clean rooms, emergency filtration systems for radioactive aerosols, absolutely clean air supply for aseptic fermentation processes, respiration masks, automobile air intake and exhaust filters, etc.).

The pattern of particle deposition in a fibrous filter is highly complex and intrinsically connected with the efficiency, loading capacity and permeability of the system. Therefore, rational design, optimization, operation, troubleshooting and innovation require intimate understanding and reliable analysis of the deposition process and its effects on the system variables. During an initial period, aerosol particles deposit on the collector surfaces, forming chainlike agglomerates. This phenomenon and its consequences have been analyzed for the case of particles larger than 1 μm in Payatakes (1977) assuming deposition by interception alone, and in Payatakes and Gradoń (1979) for deposition by combined inertial impaction and interception. In the present work, we deal with the important case of submicron particles, where the dominant transport mechanism is convective Brownian diffusion.

Dr. Leon Gradoń is on leave from the Chemical Engineering Department of the Technical University of Warsaw, Poland.

0001-1541-80-3516-0443-$01.35.

CONCLUSIONS AND SIGNIFICANCE

A theoretical model of aerosol deposition on fibers by convective Brownian diffusion is developed. The velocity and concentration fields around a fiber depend on the Knudsen number $Kn_f=l/a_f$, whereas the velocity and concentration fields around a target particle belonging to a dendrite depend, among other things, on a similar Knudsen number, $Kn_p=l/a_p$. For $Kn < 10^{-2}$, the continuum assumption is valid, and the nonslip condition applies. For $10^{-2} < Kn < \sim 1$ the nonslip boundary condition must be replaced by a slip flow condition. Finally, for $Kn > \sim 1$ the continuum assumption ceases to be valid; this regime is known as free molecular region, and within it the velocity and concentration fields are obtained by integration of the Fokker-Planck equation. Analytical solutions are obtained here for the three cases involving nonslip flow around fibers and nonslip, slip or free molecular flow around particles, namely, ($Kn_f < 10^{-2}$, $Kn_p < 10^{-2}$), ($Kn_f < 10^{-2}$, $10^{-2} < Kn_p < 1$) and ($Kn_f < 10^{-2}$, $1 < Kn_p$). These solutions cover all cases involving submicron particles and fibers with $a_f > 1\mu$m.

The theory is valid during the first and second stages of filtration (Payatakes, 1977), that is, almost up to the point where dendrites start intermeshing with their neighbors. One of the most important features of deposition by convective Brownian diffusion is that dendrites grow on the entire surface of the fiber. In the case of deposition by inertial impaction and/or interception, dendrites grow only on the forward half of the fiber or part thereof.

The importance of the dendritic pattern of aerosol particle deposition has been recognized, and several of the relevant phenomena have been studied in a number of previous works. The first experimental study was made by Billings (1966). Other experimental studies were published recently by Tien, Wang and Barot (1977), Beizaie, Wang and Tien (1979) and Bhutra and Payatakes (1979). The first theoretical study of the phenomenon by Payatakes and Tien (1976) was of deterministic nature, aiming at the prediction of the expected or average behavior of the dendritic deposits as a function of time and position on the fiber as well as of the system parameters. Improvements and extensions of the original deterministic model followed in a series of publications: Payatakes (1976*a*, *b*, 1977) and Payatakes and Gradoń (1980).

In parallel with the development of deterministic models, a series of publications appeared in which a stochastic (or Monte Carlo) approach was taken: Tien, Wang and Barot (1977), Wang, Beizaie and Tien (1977), Beizaie, Wang and Tien (1979) and Kanaoka, Emi and Myojo (1978).

Both approaches have their advantages and disadvantages, and both are capable of predicting well the relevant phenomena from basic principles. The present work is an extension of the deterministic model to the domain of submicron particles, where the main transport mechanism is convective Brownian diffusion. This is perhaps the case in which the deterministic approach has a clear advantage, as it provides an analytical solution, whereas it would be difficult and time consuming to employ stochastic simulation methods to solve this problem.

SINGLE DENDRITE GROWTH MODEL

The starting point in our theoretical modeling will be idealization of the dendrites, as described in Payatakes and Tien (1976) and Payatakes (1977). According to this idealization, dendrites are composed of particles that belong to distinct layers, and the object of the model is to express the expected number of particles in the k^{th} layer of a dendrite m_k as a function of dendrite age t, angular coordinate θ and of the system variables. For a given dendrite we set

$$\frac{dm_k}{dt} = R^{(\theta)}_{k-1,k} + R^{(\theta)}_{k,k} + R^{(\theta)}_{k+1,k} + R^{(r)}_{k-1,k} + R^{(r)}_{k,k} + R^{(r)}_{k+1,k} \quad (1)$$

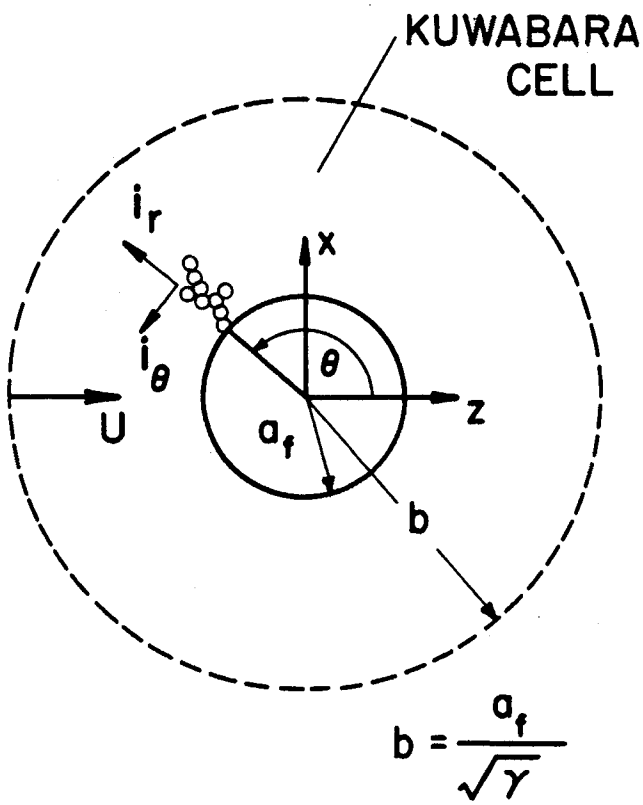

Figure 1. Kuwabara cell for a fibrous medium. Cartesian and cylindrical coordinates.

where $R_{i,k}^{(s)}$ is the rate of increase of m_k by deposition on particles occupying the i^{th} layer due to the flow component in the s direction ($s=\theta$, or r), Figure 1. Equation (1) contains two terms more than the corresponding rate equation in the cases of deposition by inertial impaction and/or interception. These terms, namely, $R_{k+1,k}^{(\theta)}$ and $R_{k+1,k}^{(r)}$, were neglected in earlier works because they are relatively small in the absence of diffusional transport. Here, of course, they must be retained, as the dominant transport mechanism is diffusion.

Proceeding with the formulation, we set

$$\left.\begin{aligned} R_{0,1}^{(\theta)} &= 0 \\ R_{k-1,k}^{(\theta)} &= \alpha\phi_{k-1,k}^{(\theta)}\, m_{k-1}\left(1-\frac{m_k}{\rho m_{k-1}}\right) \quad \text{for } k=2,3,\ldots \end{aligned}\right\} \tag{2}$$

$$R_{k,k}^{(\theta)} = \alpha\phi_{k,k}^{(\theta)}\, m_k \qquad \text{for } k=1,2,3,\ldots \tag{3}$$

$$\left.\begin{aligned} R_{2,1}^{(\theta)} &= 0 \\ R_{k+1,k}^{(\theta)} &= \alpha\phi_{k+1,k}^{(\theta)}\, m_{k+1}\left(1-\frac{m_k}{\rho m_{k+1}}\right) \quad \text{for } k=2,3,\ldots \end{aligned}\right\} \tag{4}$$

$$\left.\begin{aligned} R_{0,1}^{(r)} &= 0 \\ R_{k-1,k}^{(r)} &= \alpha\phi_{k-1,k}^{(r)}\, m_{k-1}\left(1-\frac{m_k}{\rho m_{k-1}}\right) \quad \text{for } k=2,3,\ldots \end{aligned}\right\} \tag{5}$$

$$R_{k,k}^{(r)} = \alpha\phi_{k,k}^{(r)}\, m_k \quad \text{for } k=1,2,3,\ldots \tag{6}$$

$$\left.\begin{aligned} R_{2,1}^{(r)} &= 0 \\ R_{k+1,k}^{(r)} &= \alpha\phi_{k+1,k}^{(r)}\, m_{k+1}\left(1-\frac{m_k}{\rho m_{k+1}}\right) \quad \text{for } k=2,3,\ldots \end{aligned}\right\} \tag{7}$$

where α is given by

$$\alpha = 2a_f U n_0 \tag{8}$$

As in previous works, $\phi_{k,i}^{(s)}$ is the fraction of α expected to collide, owing to the s ($s=\theta$, or r) component of the velocity, with a particle occupying the k^{th} layer of the dendrite to become part of the i^{th} layer. Finally, ρ is the coordination number, namely, the maximum number of particles in a given layer that can be attached to one and the same particle in an adjacent layer.

Equations (1) through (8) combined give

$$\frac{d\underline{m}}{dt} = \alpha\underline{\underline{A}}\,\underline{m} \tag{9}$$

where $\underline{m}$ is the vector with elements $m_1, m_2, \ldots, m_M$, and $\underline{\underline{A}}$ is a matrix defined by

$$\underline{\underline{A}} = \begin{bmatrix} b_1 & 0 & 0 & 0 & \cdots & 0 & 0 & 0 \\ a_2 & b_2 & c_2 & 0 & \cdots & 0 & 0 & 0 \\ 0 & a_3 & b_3 & c_3 & \cdots & 0 & 0 & 0 \\ | & & & & & & & \\ 0 & 0 & 0 & 0 & \cdots & a_{M-1} & b_{M-1} & c_{M-1} \\ 0 & 0 & 0 & 0 & \cdots & 0 & a_M & b_M \end{bmatrix} \tag{10}$$

where $M(\theta)$ is an integer function of θ defined by

$$m_{M+j}(\tau_f;\theta) \le \epsilon < m_M(\tau_f;\theta) \quad j=1,2,\ldots \tag{11}$$

where τ_f is the duration of the filtration run (during which the present model applies), and ϵ is a small positive number, say $\epsilon = 0.05$. The matrix elements are defined by

$$a_k = \phi_{k-1,k}^{(\theta)} + \phi_{k-1,k}^{(r)} \quad \text{for } k=2,3,\ldots \tag{12}$$

$$\left.\begin{aligned} b_1 &= \phi_{1,1}^{(\theta)} + \phi_{1,1}^{(r)} \\ b_k &= \phi_{k,k}^{(\theta)} + \phi_{k,k}^{(r)} - \frac{1}{\rho}\left[\phi_{k-1,k}^{(\theta)} + \phi_{k+1,k}^{(\theta)} + \phi_{k-1,k}^{(r)} + \phi_{k+1,k}^{(r)}\right] \quad \text{for } k=2,3,\ldots \end{aligned}\right\} \tag{13}$$

$$c_k = \phi_{k+1,k}^{(\theta)} + \phi_{k+1,k}^{(r)} \quad \text{for } k=2,3,\ldots \tag{14}$$

Note that the rate of growth of m_k depends on m_{k+1}. This creates a closure problem which was solved in the above by setting $m_{M+1}=0$ in the last equation ($k=M$). This is an acceptable approximation, in view of the definition of M [see Equation (11)].

Let $\lambda_1, \lambda_2, \ldots, \lambda_M$ be the eigenvalues of the matrix $\underline{\underline{A}}$; let, further, $\underline{u}_1, \underline{u}_2, \ldots, \underline{u}_M$ be the respective eigenvectors and let $\underline{y}_1^T, \underline{y}_2^T, \ldots, \underline{y}_M^T$ be the eigenrows. These can be determined readily with standard methods, once $\{a_k\}$, $\{b_k\}$ and $\{c_k\}$ are available. Note that $\lambda_1 = b_1$ and that the nature of the problem at hand indicates that all eigenvalues are real (as complex eigenvalues would imply oscillatory dendrite growth).

The solution of Equation (9), with initial condition given by

$$\underline{m} = \underline{m}_0 \equiv \begin{bmatrix} 1 \\ 0 \\ 0 \\ . \\ . \\ . \\ 0 \end{bmatrix} \qquad \text{at } t=0 \tag{15}$$

is

$$\underline{m}(t;\theta) = \sum_{i=1}^{M(\theta)} \frac{\underline{y}_i^T(\theta)\,\underline{m}_0}{\underline{y}_i^T(\theta)\,\underline{u}_i(\theta)}\,\underline{u}_i(\theta)\exp[\alpha\lambda_i(\theta)t] \tag{16}$$

Expressions for a_k, b_k and c_k, applying to the case of particle transport by convective Brownian diffusion, are derived below.

DETERMINATION OF a_k, b_k AND c_k

To determine a_k, b_k and c_k from Equations (12) to (14), it suffices to derive expressions for $\phi_{i,k}^{(s)}$, for $i = k-1, k$ and $k+1$ and $s = r$ and θ.

An exact calculation of these quantities does not seem practical (or even feasible), considering the complications arising from the proximity of the collector and neighboring particles and from the random shape of the dendrites. However, approximate expressions can be obtained with the method described presently. We begin by outlining the general approach, and then we enumerate specific results.

To calculate $\phi_{k,i}^{(r)}$, we assume that a target particle in the k^{th} layer is immersed in an unbounded uniform flow with approach velocity $U_k^{(r)}$ and approach particle number concentration n_{ok}, Figure 2. These two variables are assumed to have the values that would prevail at the location of the center of the target particle in the absence of any dendrites; accordingly

$$U_k^{(r)} = \left|v_r[a_f + (2k-1)a_p, \theta]\right| \tag{17}$$

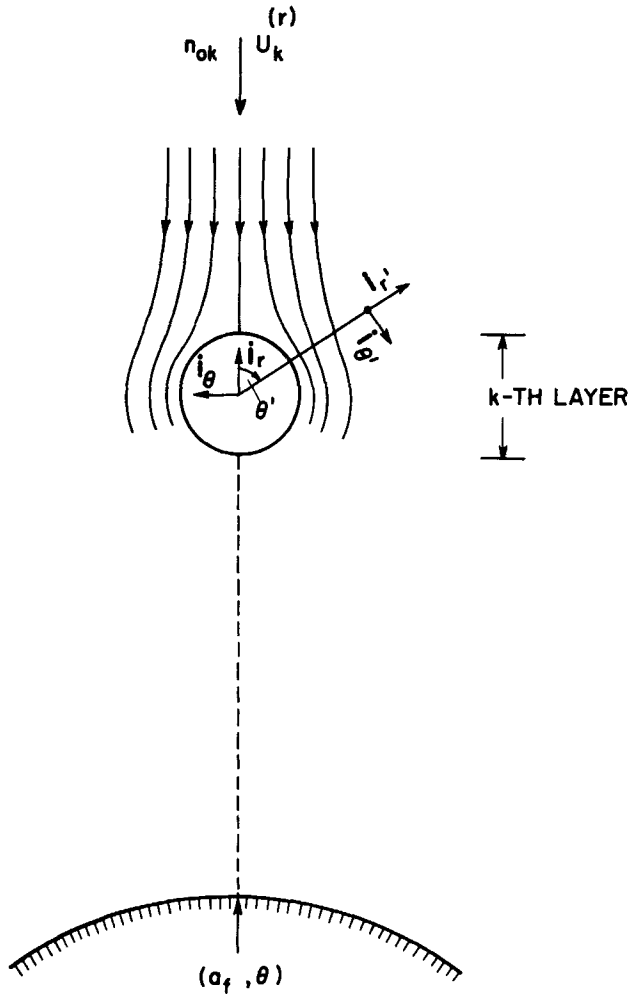

Figure 2. Assumed flow around a particle in the k^{th} layer, due to the radial component of the main flow, and system of coordinates.

$$n_{ok} = n\,[a_f + (2k-1)\,a_p,\ \theta] \tag{18}$$

In the above, v_r is the radial component of the unperturbed velocity around the collector, and n is the corresponding number concentration, obtained by assuming that the cylindrical surface $r = a_f + a_p$ is an adsorbing boundary $[n(a_f + a_p, \theta) = 0]$. Assuming, now, that the spherical surface $r' = 2a_p$ surrounding the target particle is also an adsorbing boundary and ignoring the presence of the fiber, one can derive the corresponding concentration field, $n_k^{(r)}(r', \theta')$.*. Then, the particle flux density normal to the target particle wall is obtained readily from

$$j_k^{(r)}(\theta') = -D\frac{\partial n_k^{(r)}}{\partial r'}\Big)_{r' = 2a_p} \tag{19}$$

where D is given by

$$D = \frac{kT}{6\pi\mu a_p} C_s \tag{20}$$

where C_s is given by

$$C_s = 1 + 1.257\,Kn_p + 0.400\,Kn_p \exp(-1.10/Kn_p) \tag{21}$$

* θ' is measured from the forward stagnation point, Figure 2.

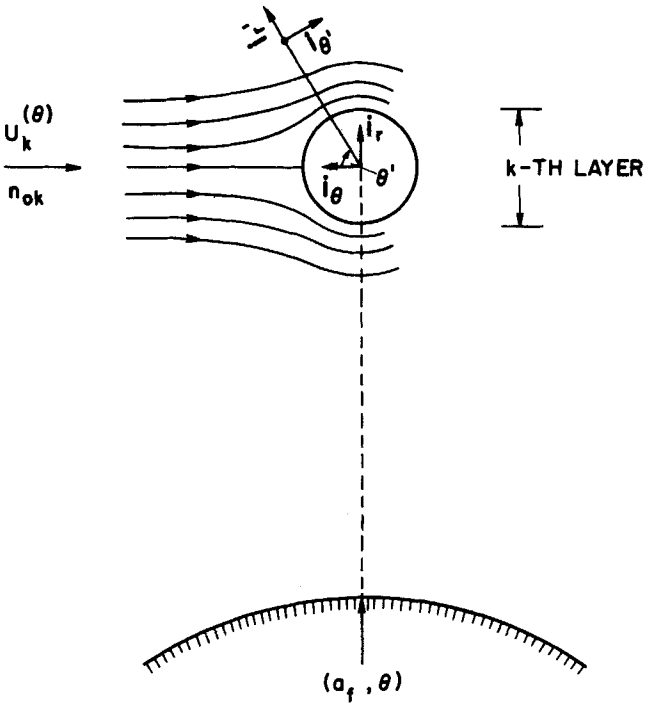

Figure 3. Assumed flow around a particle in the k^{th} layer, due to the tangential component of the main flow, and system of coordinates.

If we recall the definition of $\phi_{k,i}^{(r)}$, it becomes clear that $\alpha\phi_{k,i}^{(r)}$ is the rate at which particles deposit on a k^{th} layer particle, at locations that make them members of the i^{th} layer. Consequently

$$\phi_{k,k+1}^{(r)} = -\frac{8\pi a_p^2}{\alpha}\int_0^{\pi/3} j_k^{(r)}(\theta')\sin\theta'\,d\theta' \quad \text{for}\ \frac{\pi}{2} \le \theta \le \pi$$

$$\phi_{k,k+1}^{(r)} = -\frac{8\pi a_p^2}{\alpha}\int_{2\pi/3}^{\pi} j_k^{(r)}(\theta')\sin\theta'\,d\theta' \quad \text{for}\ 0 \le \theta \le \frac{\pi}{2} \tag{22}$$

$$\phi_{k,k}^{(r)} = -\frac{8\pi a_p^2}{\alpha}\int_{\pi/3}^{2\pi/3} j_k^{(r)}(\theta')\sin\theta'\,d\theta' \quad \text{for}\ 0 \le \theta \le \pi \tag{23}$$

$$\phi_{k,k-1}^{(r)} = -\frac{8\pi a_p^2}{\alpha}\int_{2\pi/3}^{\pi} j_k^{(r)}(\theta')\sin\theta'\,d\theta' \quad \text{for}\ \frac{\pi}{2} \le \theta \le \pi$$

$$\phi_{k,k-1}^{(r)} = -\frac{8\pi a_p^2}{\alpha}\int_0^{\pi/3} j_k^{(r)}(\theta')\sin\theta'\,d\theta' \quad \text{for}\ 0 \le \theta \le \frac{\pi}{2} \tag{24}$$

Similarly, to calculate $\phi_{k,i}^{(\theta)}$, we assume that the target particle in the k^{th} layer is immersed in an unbounded uniform flow with approach velocity $U_k^{(\theta)}$ and approach particle number concentration n_{ok}, Figure 3. The approach velocity is given by

$$U_k^{(\theta)} = |v_\theta\,[a_f + (2k-1)a_p, \theta]| \tag{25}$$

As before, n_{ok} is given by Equation (18). Assuming that the spherical surface $r' = 2a_p$ surrounding the target particle is an adsorbing boundary, one can derive the corresponding field $n_k^{(\theta)}(r', \theta')$ and the flux density normal to the wall:

$$j_k^{(\theta)}(\theta') = -D\frac{\partial n_k^{(\theta)}}{\partial r'}\Big)_{r' = 2a_p} \tag{26}$$

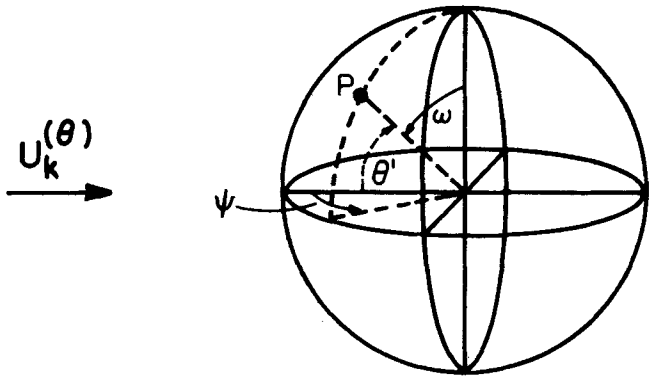

Figure 4. Variables used in calculating the particle fluxes in Equations (27) to (29).

It is relatively easy then to show that $\phi_{k,i}^{(\theta)}$ are given by

$$\phi_{k,k+1}^{(\theta)} = -\frac{8a_p^2}{\alpha}\int_0^{\pi/3}\left(\int_0^{\pi} j_k^{(\theta)}[\theta'(\omega,\psi)]\,d\psi\right)\sin\omega\,d\omega \tag{27}$$

$$\phi_{k,k}^{(\theta)} = -\frac{16a_p^2}{\alpha}\int_{\pi/3}^{\pi/2}\left(\int_0^{\pi} j_k^{(\theta)}[\theta'(\omega,\psi)]\,d\psi\right)\sin\omega\,d\omega \tag{28}$$

$$\phi_{k,k-1}^{(\theta)} = -\frac{8a_p^2}{\alpha}\int_{2\pi/3}^{\pi}\left(\int_0^{\pi} j_k^{(\theta)}[\theta'(\omega;\psi)]\,d\psi\right)\sin\omega\,d\omega \tag{29}$$

where the argument θ' of $j_k^{(\theta)}$ in the integrands depends on the dummy variables ω and ψ through the expression (see Figure 4)

$$\theta' = \arccos(\sin\omega\,\cos\psi)$$

At this point, the problem of calculating $\phi_{k,i}^{(s)}$ has been reduced to that of determining the particle flux densities $j_k^{(r)}$ and $j_k^{(\theta)}$.

In the present work, we shall restrict our attention to the case of nonslip flow around the collector ($Kn_f < 10^{-2}$). The streamfunction for nonslip flow can be expressed as (Kirsh and Stechkina, 1978):

$$\psi \cong -\frac{Ua_f}{2K}\left(2\frac{r}{a_f}\ln\frac{r}{a_f} - \frac{r}{a_f} + \frac{a_f}{r}\right)\sin\theta \tag{30}$$

where K depends on the flow model. Specifically,

$$K = 2 - \ln Re_f \qquad \text{(Lamb, 1945)} \tag{31}$$

$$K = -\frac{1}{2}\ln\gamma - \frac{1}{2} + \gamma^2/(1+\gamma^2) \qquad \text{(Happel, 1958)} \tag{31a}$$

$$K = -\frac{1}{2}\ln\gamma - \frac{3}{4} + \gamma - \frac{1}{4}\gamma^2 \qquad \text{(Kuwabara, 1959)} \tag{31b}$$

The angular coordinate θ is measured from the downstream stagnation point. The Lamb solution pertains to unbounded flow with uniform approach velocity and is based on Oseen's equation. The Happel and Kuwabara models apply to creeping flow through random arrays of parallel fibers having packing density γ.

The corresponding velocity components are given by

$$v_r \cong \frac{U}{2K}\left[2\ln\frac{r}{a_f} - 1 + \left(\frac{a_f}{r}\right)^2\right]\cos\theta \tag{32}$$

$$v_\theta \cong -\frac{U}{2K}\left[2\ln\frac{r}{a_f} + 1 - \left(\frac{a_f}{r}\right)^2\right]\sin\theta \tag{33}$$

Assuming that the cylindrical surface is an adsorbing boundary, and taking in account the finite dimension of the aerosol particles, we obtain the following particle number concentration

$$\frac{n(r,\theta)}{n_o} = 0.870\int_0^{w}\exp\left(-\frac{4}{9}z^3\right)dz \tag{34}$$

with

$$w = \left(\frac{r}{a_f} - 1 - R\right)\left(\frac{Pe_f}{2K}\right)^{1/3}\frac{\sqrt{\sin\theta}}{\left(2\int_0^{\pi-\theta}\sqrt{\sin\phi}\,d\phi\right)^{1/3}} \tag{34a}$$

where $Pe_f = 2a_fU/D$, and $R = a_p/a_f$.

This solution was obtained by Natanson (1975) using the method developed originally by Levich (see Levich 1962). Note that for $r = a_f + a_p$, we have $n = 0$ and that as $r \to \infty$, $n \to n_o$.

The particle flux density on the fiber wall is given by

$$j(\theta) = -D\frac{\partial n}{\partial r}\Big)_{r=a_f+a_p} = -0.870\left(\frac{n_oD}{a_f}\right)\left(\frac{Pe_f}{2K}\right)^{1/3}\frac{\sqrt{\sin\theta}}{\left(2\int_0^{\pi-\theta}\sqrt{\sin\phi}\,d\phi\right)^{1/3}} \tag{35}$$

Equations (17), (25) and (18) in conjunction with (32), (33) and (34) give $U_k^{(r)}$, $U_k^{(\theta)}$ and n_{ok} for all values of k. At this point we are ready to calculate the rate of diffusional deposition on a target particle in the k^{th} layer. The solution to the latter problem depends on the magnitude of the relevant Knudsen number, Kn_p. Analytical expressions for the number concentration and flux density on a sphere wall for nonslip, slip and free molecular flow are given in the appendix. The solutions for slip and free molecular flow are new and were extracted from the results of Gradoń and Payatakes (1980).

Based on the results summarized in the appendix and using Equations (22) to (24) and (27) to (29), we obtain the following expressions:

Case 1: nonslip flow around fibers ($Kn_f < 10^{-2}$); nonslip flow around particles ($Kn_p < 10^{-2}$)

$$\left.\begin{aligned}\phi_{k,k+1}^{(r)} &= 8.56a_p\Phi_k^{(r)} \quad \text{for } \frac{\pi}{2} \le \theta \le \pi\\ \phi_{k,k+1}^{(r)} &= 3.42a_p\Phi_k^{(r)} \quad \text{for } 0 \le \theta \le \frac{\pi}{2}\end{aligned}\right\} \tag{36}$$

$$\phi_{k,k}^{(r)} = 13.39a_p\Phi_k^{(r)} \quad \text{for } 0 \le \theta \le \pi \tag{37}$$

$$\left.\begin{aligned}\phi_{k,k-1}^{(r)} &= 3.42a_p\Phi_k^{(r)} \quad \text{for } \frac{\pi}{2} \le \theta \le \pi\\ \phi_{k,k-1}^{(r)} &= 8.56a_p\Phi_k^{(r)} \quad \text{for } 0 \le \theta \le \frac{\pi}{2}\end{aligned}\right\} \tag{38}$$

$$\phi_{k,k+1}^{(\theta)} = 6.52\,a_p\Phi_k^{(\theta)} \quad \text{for } 0 \le \theta \le \pi \tag{39}$$

$$\phi_{k,k}^{(\theta)} = 12.33\, a_p \Phi_k^{(\theta)} \quad \text{for } 0 \le \theta \le \pi \tag{40}$$

$$\phi_{k,k-1}^{(\theta)} = 6.52\, a_p \Phi_k^{(\theta)} \quad \text{for } 0 \le \theta \le \pi \tag{41}$$

where

$$\Phi_k^{(r)} = Pe_f^{-1}\, Pe_{pk}^{(r)\,1/3}\, \frac{n_{ok}}{n_o} \tag{42}$$

$$\Phi_k^{(\theta)} = Pe_f^{-1}\, Pe_{pk}^{(\theta)\,1/3}\, \frac{n_{ok}}{n_o} \tag{43}$$

with

$$Pe_f = \frac{2a_f U}{D} \tag{44}$$

$$Pe_{pk}^{(r)} = \frac{2a_p U_k^{(r)}}{D} \tag{45}$$

$$Pe_{pk}^{(\theta)} = \frac{2a_p U_k^{(\theta)}}{D} \tag{46}$$

$$U_k^{(r)} = \frac{U}{2K}\left(2\ln X_k - 1 + X_k^{-2}\right)\left|\cos\theta\right| \tag{47}$$

$$U_k^{(\theta)} = \frac{U}{2K}\left(2\ln X_k + 1 - X_k^{-2}\right)\sin\theta \tag{48}$$

$$X_k = 1 + (2k-1)R \tag{49}$$

and where

$$\frac{n_{ok}}{n_o} = 0.870 \int_0^{w_k} \exp\left(-\frac{4}{9}z^3\right) dz \tag{50}$$

with

$$w_1 = R\left(\frac{Pe_f}{2K}\right)^{1/3} \frac{\sqrt{\sin\theta}}{\left(2\int_0^{\pi-\theta}\sqrt{\sin\phi}\, d\phi\right)^{1/3}} \tag{50a}$$

$$w_k = 2(k-1)\, R\left(\frac{Pe_f}{2K}\right)^{1/3} \frac{\sqrt{\sin\theta}}{\left(2\int_0^{\pi-\theta}\sqrt{\sin\phi}\, d\phi\right)^{1/3}}; \quad k=2,3\ldots$$

Case 2: nonslip flow around fibers ($Kn_f < 10^{-2}$); slip flow around particles ($10^{-2} < Kn_p < \sim 1$)

$$\left.\begin{aligned} \phi_{k,k+1}^{(r)} &= 8.56\, a_p\, \Phi_k^{(r)}\, S_p^{1/3} \quad \text{for } \frac{\pi}{2} \le \theta \le \pi \\ \phi_{k,k+1}^{(r)} &= 3.42\, a_p\, \Phi_k^{(r)}\, S_p^{1/3} \quad \text{for } 0 \le \theta \le \frac{\pi}{2} \end{aligned}\right\} \tag{51}$$

$$\phi_{k,k}^{(r)} = 13.39\, a_p\, \Phi_k^{(r)}\, S_p^{1/3} \quad \text{for } 0 \le \theta \le \pi \tag{52}$$

$$\left.\begin{aligned} \phi_{k,k-1}^{(r)} &= 3.42\, a_p\, \Phi_k^{(r)}\, S_p^{1/3} \quad \text{for } \frac{\pi}{2} \le \theta \le \pi \\ \phi_{k,k-1}^{(r)} &= 8.56\, a_p\, \Phi_k^{(\theta)}\, S_p^{1/3} \quad \text{for } 0 \le \theta \le \frac{\pi}{2} \end{aligned}\right\} \tag{53}$$

$$\phi_{k,k+1}^{(\theta)} = 6.52\, a_p\, \Phi_k^{(\theta)}\, S_p^{1/3} \quad \text{for } 0 \le \theta \le \pi \tag{54}$$

$$\phi_{k,k}^{(\theta)} = 12.33\, a_p\, \Phi_k^{(\theta)}\, S_p^{1/3} \quad \text{for } 0 \le \theta \le \pi \tag{55}$$

$$\phi_{k,k-1}^{(\theta)} = 6.52\, a_p\, \Phi_k^{(\theta)}\, S_p^{1/3} \quad \text{for } 0 \le \theta \le \pi \tag{56}$$

where , as before, $\Phi_k^{(r)}$ and $\Phi_k^{(\theta)}$ are given by Equations (42), (43) and (50). The dimensionless coefficient S_p is defined by

$$S_p = \frac{1 + 2(\beta/a_p)}{1 + 3(\beta/a_p)} = \frac{1 + 2(\beta/l)Kn_p}{1 + 3(\beta/l)Kn_p} \tag{57}$$

and accounts for the effect of slip on the rate of deposition. Rigorous analysis of the effect of discontinuity in the tangential velocity at the surface of a particle (Epstein, 1924; see also Fuchs, 1964) shows that the slip coefficient β is given by

$$\beta = 0.7004\left(\frac{2}{\kappa} - 1\right) l \tag{58}$$

Based on experimental results by Millikan and others, Fuchs (1964) suggests that in practice $\beta/l = 0.86$ ($\kappa = 0.90$) may be taken for liquid droplets and very smooth solid spheres and $\beta/l = 0.70$ ($\kappa = 1.0$) for rough spheres. As can be seen, surface rougness results in nearly complete diffuse reflection of gas molecules.

Note that for small values of the particle Knudsen number, S_p tends to unity, and Equations (51) to (56) reduce to Equations (36) to (41), respectively.

Case 3: nonslip flow around fibers ($Kn_f < 10^{-2}$); free molecular flow around particles ($\sim 1 < Kn_p$)

$$\left.\begin{aligned} \phi_{k,k+1}^{(r)} &= a_p J_1 \Psi_k \quad \text{for } \frac{\pi}{2} \le \theta \le \pi \\ \phi_{k,k+1}^{(r)} &= a_p J_{-1} \Psi_k \quad \text{for } 0 \le \theta \le \frac{\pi}{2} \end{aligned}\right\} \tag{59}$$

$$\phi_{k,k}^{(r)} = a_p J_o \Psi_k \quad \text{for } 0 \le \theta \le \pi \tag{60}$$

$$\left.\begin{aligned} \phi_{k,k-1}^{(r)} &= a_p J_{-1} \Psi_k \quad \text{for } \frac{\pi}{2} \le \theta \le \pi \\ \phi_{k,k-1}^{(r)} &= a_p J_1 \Psi_k \quad \text{for } 0 \le \theta \le \frac{\pi}{2} \end{aligned}\right\} \tag{61}$$

$$\phi_{k,k+1}^{(\theta)} = a_p I_1 \Psi_k \quad \text{for } 0 \le \theta \le \pi \tag{62}$$

$$\phi_{k,k}^{(\theta)} = a_p I_o \Psi_k \quad \text{for } 0 \le \theta \le \pi \tag{63}$$

$$\phi_{k,k-1}^{(\theta)} = a_p I_{-1} \Psi_k \quad \text{for } 0 \le \theta \le \pi \tag{64}$$

where

$$\Psi_k = 4\pi A\, Pe_f^{-1}\, \frac{n_{ok}}{n_o} \tag{65}$$

$$J_1 = \frac{1}{4} + \frac{1}{2St_{pk}^{(r)}} \ln \frac{\left(1 - \frac{1}{2}St_{pk}^{(r)}\right)}{\left(1 - St_{pk}^{(r)}\right)} \tag{66}$$

$$J_o = \frac{1}{2} + \frac{1}{2St_{pk}^{(r)}} \ln \frac{\left(2 + St_{pk}^{(r)}\right)}{\left(2 - St_{pk}^{(r)}\right)} \tag{67}$$

$$J_{-1} = \frac{1}{4} + \frac{1}{2St_{pk}^{(r)}} \ln \frac{\left(1 + St_{pk}^{(r)}\right)}{\left(1 + \frac{1}{2}St_{pk}^{(r)}\right)} \tag{68}$$

$$I_1 = I_{-1} = \frac{1}{\pi}\int_0^{\pi/3}\left(\int_0^{\pi} \frac{1 - \frac{1}{2}St_{pk}^{(\theta)}\sin\omega\cos\psi}{1 - St_{pk}^{(\theta)}\sin\omega\cos\psi}\, d\psi\right)$$

TABLE 1. CALCULATED VALUES OF $J_1, J_o, J_{-1}, I_1, I_o$ AND I_{-1} FOR TYPICAL VALUES OF St_{pk}

St_{pk}	J_1	J_o	J_{-1}	I_1	I_o	I_{-1}	$J_1+J_o+J_{-1}$ $(=I_1+I_o+I_{-1})$
0	0.5	1.0	0.5	0.5	1.0	0.5	2.0
0.001	0.5002	1.0000	0.4998	0.500	1.000	0.500	2.0000
0.01	0.5019	1.0000	0.4981	0.500	1.000	0.500	2.0000
0.1	0.5203	1.0004	0.4826	0.501	1.002	0.501	2.0033
0.5	0.6555	1.0108	0.4323	0.508	1.083	0.508	2.0986

$$\sin\omega\, d\omega \qquad (69)$$

$$I_0 = \frac{2}{\pi}\int_{\pi/3}^{\pi/2}\left(\int_0^{\pi}\frac{1-\frac{1}{2}St_{pk}^{(\theta)}\sin\omega\cos\psi}{1-St_{pk}^{(\theta)}\sin\omega\cos\psi}\,d\psi\right)$$

$$\sin\omega\, d\omega \qquad (70)$$

$$St_{pk}^{(r)} = \frac{2a_p\rho_p U_k^{(r)}}{9\mu}C_s \qquad (71)$$

$$St_{pk}^{(\theta)} = \frac{2a_p\rho_p U_k^{(\theta)}}{9\mu}C_s \qquad (72)$$

Here too, n_{ok}/n_o, $U_k^{(r)}$ and $U_k^{(\theta)}$ are given by Equations (50), (47) and (48), respectively.

Calculated values of the coefficients $J_1, J_o, J_{-1}, I_1, I_o$ and I_{-1} for various values of St_{pk} are given in Table 1. As can be seen, these coefficients are rather weak functions of St_{pk}, and for $St_{pk}<0.01$ can be replaced by constants. In the molecular flow region, we have $a_p<l$, and so Equations (71) and (72) give St_{pk} values which are quite smaller than unity. The following simple expressions can be used for, say, $St_{pk}<0.5$:

$$J_1 = 0.5 + St_{pk}^{(r)}[0.18 + 0.26\,St_{pk}^{(r)}] \qquad (73)$$

$$J_o = 1.0 + 0.04\,St_{pk}^{(r)2} \qquad (74)$$

$$J_{-1} = 0.5 - St_{pk}^{(r)}[0.18 - 0.09\,St_{pk}^{(r)}] \qquad (75)$$

$$I_1 = I_{-1} = 0.5 + St_{pk}^{(\theta)}[0.008 + 0.016\,St_{pk}^{(\theta)}] \qquad (76)$$

$$I_o = 1.0 + 0.3\,St_{pk}^{(\theta)2} \qquad (77)$$

The effects of increasing St_{pk} on the rate and pattern of particle deposition can be seen by inspecting the values of J_1, J_{-1} and $(J_1+J_o+J_{-1})$, Table 1. The total rate of deposition is proportional to $(J_1+J_o+J_{-1})$; it increases with St_{pk}, but very slowly. On the other hand, the rate of deposition on the upstream part of the target particle $(0 \le \theta' \le \pi/3)$ is proportional to J_1, and it increases significantly with St_{pk}. This increase is accompanied by a decrease of the rate of deposition on the downstream part of the target particle $(2\pi/3 \le \theta' \le \pi)$, as shown by the values of J_{-1}. Deposition on the midsection of the particle $(\pi/3 \le \theta' \le 2\pi/3)$ is proportional to J_o and remains nearly constant. This lack of symmetry is due to molecular drift, represented by nonvanishing St_{pk} values. For $St_{pk} = 0$, deposition becomes symmetrical. In the latter situation, our solution agrees with those obtained by Astakhov (1965) and Sitarski and Seinfeld (1977) for negligible drift.

TABLE 2. CALCULATED VALUES OF $\nu_o(\theta)$

$(\pi-\theta)$	ν_0	$(\pi-\theta)$	ν_0
0	0.433	1.6	0.348
0.2	0.429	1.8	0.327
0.4	0.422	2.0	0.301
0.6	0.416	2.2	0.273
0.8	0.408	2.4	0.243
1.0	0.396	2.6	0.206
1.2	0.383	2.8	0.165
1.4	0.366	3.0	0.103
$\pi/2$	0.352	π	0

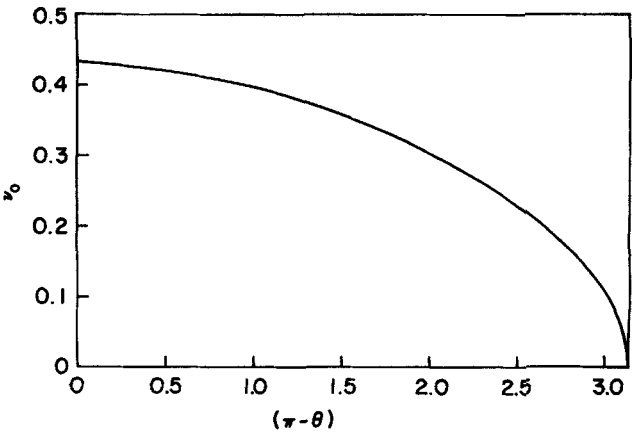

Figure 5. Plot of calculated ν_0 values vs. $(\pi-\theta)$. The forward stagnation point corresponds to $\pi-\theta=0$.

DENDRITE NUMBER DISTRIBUTION FUNCTION, $N(\tau, \theta)$

This function is defined so that $N(\tau,\theta)\delta\theta$ is the number of dendrites per unit fiber length between θ and $\theta+\delta\theta$ at time τ (taking into account both sides of the fiber). Let $N_o(\tau,\theta)$ be the dendrite number distribution function that would obtain in the absence of shadow effects. A simple particle balance gives

$$N_0 = \alpha\eta_o\tau\nu_0(\theta) \qquad (78)$$

where η_o is given in the present case by

$$\eta_0 = 3.68\,(2K)^{-1/3}Pe_f^{-2/3} \qquad (79)$$

The function $\nu_0(\theta)$ is defined as

$$\nu_0 = \frac{\sqrt{\sin\theta}\Big/\left(2\int_0^{\pi-\theta}\sqrt{\sin\phi}\,d\phi\right)^{1/3}}{\int_0^{\pi}\frac{\sqrt{\sin\theta}}{\left(2\int_0^{\pi-\theta}\sqrt{\sin\phi}\,d\phi\right)^{1/3}}\,d\theta} \qquad (80)$$

Calculated values of ν_0 are given in Table 2 and plotted

in Figure 5. For computational purposes, the following simple expression is a satisfactory approximation:

$$\nu_0 = 0.433 \sin^{3/5}\frac{\theta}{2} \tag{81}$$

N_o, as given by Equation (78), overestimates somewhat the number of dendrites due to omission of the shadow effect. The latter term was coined by Tien, Wang and Barot (1977) to describe the shielding of part of the fiber area behind a given dendrite from oncoming particles. This phenomenon is particularly important when the mechanisms of deposition are inertial impaction and/or interception. Indeed, in such cases particles follow smooth trajectories, and the shadows of dendrites can be quite long; this problem was treated in Payatakes and Gradoń (1980). In the case of dominant Brownian diffusion, however, the particles follow tortuous trajectories, which tend to render the shadow effect much less important. The main effect of a deposited dendrite is that it makes a certain small area around its root inaccessible for growth of new dendrites. Since the fraction of the area of a strip $(\theta, \theta + \delta\theta)$ that is not occupied by dendrites is approximately $[1 - 2\pi\, Ra_p N]$, we have

$$\frac{\partial N}{\partial \tau} = \frac{\partial N_o}{\partial \tau}[1 - 2\pi\, Ra_p N] \tag{82}$$

Calculating $\partial N_o/\partial\tau$ from Equation (78), substituting in Equation (82) and integrating, we obtain

$$N(\tau,\theta) = \frac{1}{2\pi Ra_p}\{1 - \exp[-f\,\nu_o(\theta)\tau]\} \tag{83}$$

where f is defined by

$$f = 2\pi\, Ra_p \alpha \eta_o \tag{84}$$

Clearly, the rate of increase of the number of dendrites is a decreasing function of time everywhere.

DENDRITE AGE DISTRIBUTION FUNCTION, $\chi(t;\tau,\theta)$

Let $\chi(t;\tau,\theta)\,\delta t$ be the fraction of the population of dendrites at time τ and at angle θ that have ages between t and $t+\delta t$. It is simple to show that during the unhindered dendrite growth period we have

$$\chi(t;\tau,\theta) = \frac{\dfrac{\partial N(\tau - t,\theta)}{\partial \tau}}{\displaystyle\int_0^\tau \frac{\partial N(\tau',\theta)}{\partial \tau'} d\tau'} \quad \text{for } 0 \le \tau \le \tau_{ug} \tag{85}$$

with

$$\tau_{ug} \cong \frac{\pi}{100 a_p^2 U n_o \eta_0} \tag{86}$$

Equations (83) and (85) give

$$\chi(t;\tau,\theta) = \frac{f\nu_0(\theta)\exp[-f\nu_0(\theta)(\tau - t)]}{\{1 - \exp[-f\nu_0(\theta)\tau]\}} \quad \text{for } 0 \le \tau \le \tau_{ug} \tag{87}$$

As can be seen from the above equation, old dendrites are more numerous than younger ones. This is natural, as the presence of older dendrites impedes the formation of new ones.*

* If the shadow effect is omitted, Equation (85) gives $\chi(t;\tau,\theta)=1/\tau$, which implies that dendrites of all ages exist in the same proportion, at all times.

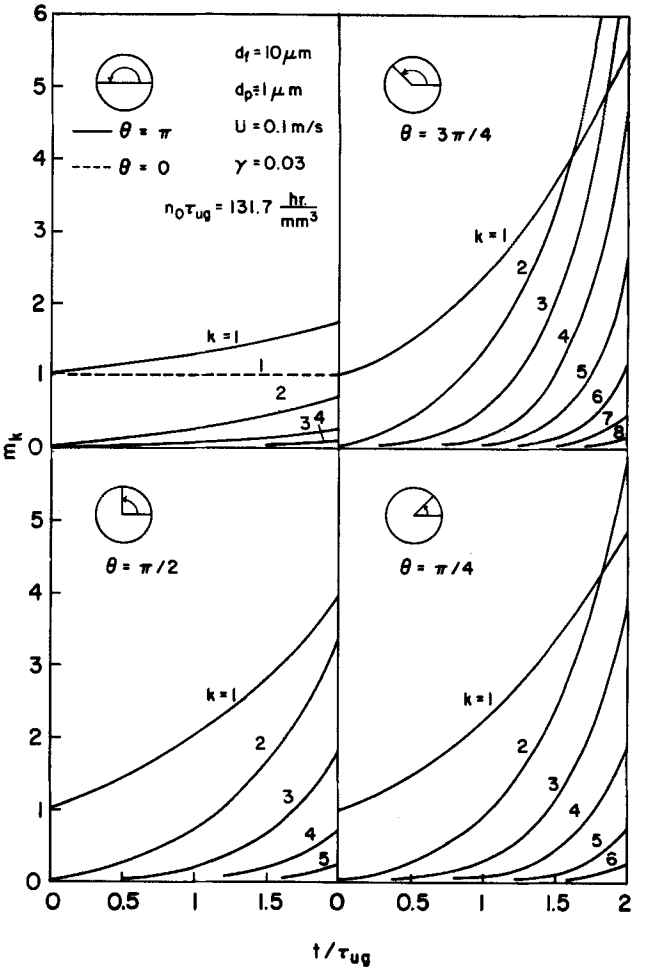

Figure 6. Calculated sample profiles of m_k for the conditions shown. Here $R=0.1$.

TRANSIENT BEHAVIOR OF A FIBROUS FILTER OF DIFFERENTIAL THICKNESS

The general dependence of the filter coefficient λ, the pressure gradient $(\partial P/\partial z)_\tau$ and the specific deposit σ on time τ and the system parameters is given by Equations (18), (20), and (31), respectively, in Payatakes (1977). Substituting into those equations the expressions for N and χ from Equations (83) and (87), we get

$$\frac{\lambda(\tau)}{\lambda_o} = 1 + \int_0^\pi \left\{ \sum_{k=1}^{M(\theta)} \left[\int_0^\tau \dot{m}_k(t;\theta) \exp[-f\nu_o(\theta)(\tau - t)]\,dt \right] \right\} \nu_o(\theta)\,d\theta \tag{88}$$

$$\frac{\left(\dfrac{\partial P}{\partial z}\right)_\tau}{\left(\dfrac{dP}{dz}\right)_{\sigma=0}} = 1 + \frac{K\alpha\eta_o}{4\pi\mu U_s} \int_0^\pi \left\{ \sum_{k=1}^{M(\theta)} \left[\int_0^\tau m_k(t;\theta) \exp[-f\nu_o(\theta)(\tau - t)]\,dt \right] F_{pk}(\theta) \right\} \nu_o(\theta)\,d\theta \tag{89}$$

$$\sigma(\tau) = \frac{4\gamma a_p^3 \alpha \eta_o}{3a_f^2} \int_0^\pi \left\{ \sum_{k=1}^{M(\theta)} \left[\int_0^\tau m_k(t;\theta) \exp[-f\nu_o(\theta)(\tau - t)]\,dt \right] \right\} \nu_o(\theta)\,d\theta \tag{90}$$

with

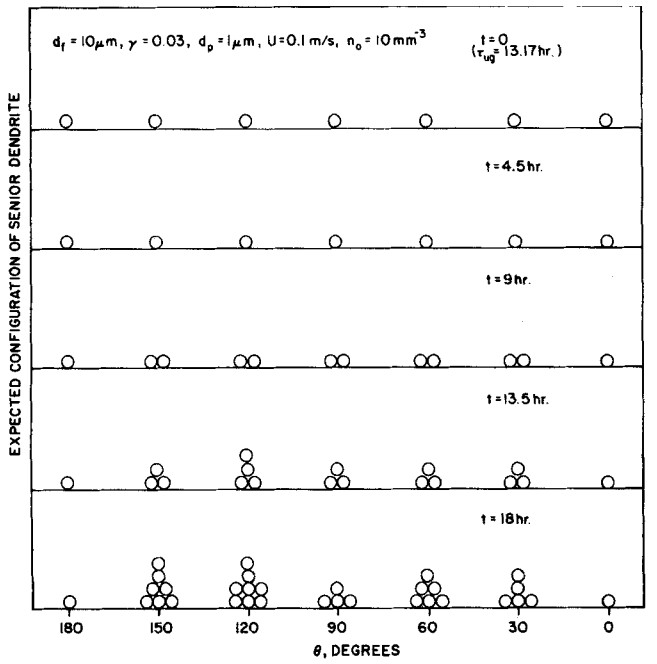

Figure 7. Two-dimensional idealized representation of the expected dendrite configuration as a function of age and position. The conditions are the same as those for Figure 6.

$$\left(\frac{dP}{dz}\right)_{\sigma=0} = -\frac{4\gamma\mu U_s}{Ka_f^2} \qquad (91)$$

TRANSIENT BEHAVIOR OF A FIBROUS FILTER OF FINITE THICKNESS

The transient behavior of a macroscopic filter can be calculated by integrating Equations (88) to (90) numerically to obtain f_λ and f_P as functions of σ, and then proceeding to integrate the system of filtration equations. The detailed procedure is given in Payatakes (1976*b*; 1977).

SAMPLE CALCULATIONS

The behavior of the model is demonstrated with sample calculations for two different systems. The parameter values for the first set of calculations are $d_f = 10\,\mu$m, $\gamma = 0.03$, $d_p = 1\mu$m, $U = 0.1$ m/s, $n_o = 10$ mm^{-3}, $\mu = 1.813 \times 10^{-5}$ Pa·s, $l = 0.083\ \mu$m, $\rho = 3$, $M(\theta) = 15$, (estimated τ_{ug} = 13.17 hr). Calculated values of m_k are shown in Figure 6 as functions of dendrite age t for five different angles, namely, $\theta = \pi$, $3\pi/4$, $\pi/2$, $\pi/4$ and 0. The corresponding expected configurations of the senior dendrites at various angular positions and times are shown in Figure 7. The parameter values for the second set of calculations are $d_f = 4\ \mu$m, $\gamma = 0.03$, $d_p = 1\ \mu$m, $U = 0.1$ m/s, $n_o = 10$ mm^{-3}, $\mu = 1.813 \times 10^{-5}$ Pa·s, $l = 0.083\ \mu$m, $\rho = 3$, $M(\theta) = 15$, (estimated τ_{ug} = 7.17 hr). The resulting m_k profiles for this set of parameters are plotted in Figure 8, and the corresponding expected configurations of the senior dendrites are shown in Figure 9. Note that the only difference in the two sets of parameters investigated is in the fiber diameter value. Owing to this difference, the interception parameter for the first system is $R = 0.1$, whereas for the second it is $R = 0.25$.

Several conclusions can be drawn from these results:

1. Under conditions of convective Brownian diffusion, dendrites are formed over the entire fiber surface.

2. The profiles $\{m_k;\ k = 1,2,3, \ldots\}$ depend strongly on the angular position. The largest dendrites are found on

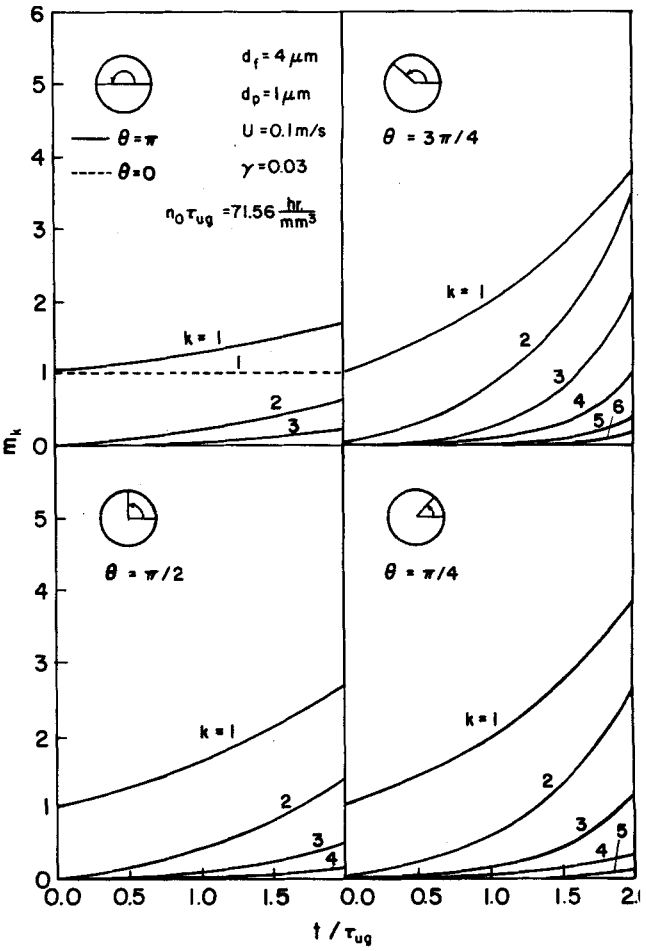

Figure 8. Calculated sample profiles of m_k for the conditions shown. Here $R = 0.25$.

the upstream part of the fiber, in the range (~135±15 deg), and its symmetric strip (~225±15 deg).

3. The senior dendrite configuration seems to be bimodal, in a certain sense. Relatively large dendrites are

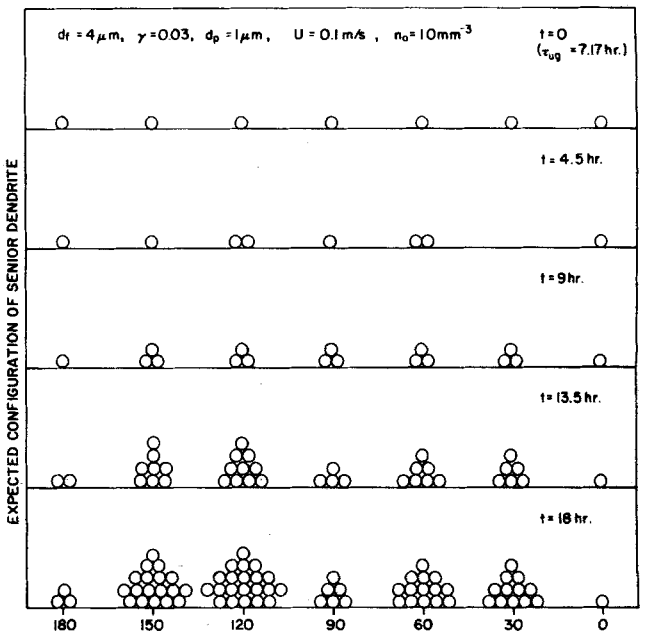

Figure 9. Two-dimensional idealized representation of the expected dendrite configuration as a function of age and position. The conditions are the same as those for Figure 8.

also found in the downstream ranges ($\sim 45 \pm 15$, $\sim 315 \pm 15$ deg). These dendrites are larger than those found at 90 and 270 deg, but not as large as the ones found around 135 and 225 deg.

4. The dendritic growth on the smaller fiber (d_f=4 μm, R=0.25) is faster than that on the larger fiber (d_f=10 μm, R=0.1). In general, larger interception parameter values lead to more pronounced dendritic deposition.

5. The configurations of these dendrites, formed through convective Brownian motion, are somewhat less slender and elongated than those formed by inertial impaction and/or interception (see Payatakes, 1977; Payatakes and Gradoń, 1980). In this connection, we should emphasize that the two-dimensional representation of dendrites in Figures 7 and 9 gives them a considerably more obese appearance than that of their three-dimensional counterparts (see also Payatakes, 1977).

6. Regardless of size or age, the number of dendrites per unit area is a monotonically decreasing function of $(\pi-\theta)$ in the range $(0,\pi)$, (see Figure 5).

ACKNOWLEDGMENTS

We thank Dr. Kikuo Okuyama of Osaka Prefecture University, Japan, for kindly providing the calculations summarized in Figures 6 to 9. Dr. Okuyama is currently visiting with the Chemical Engineering Department of the University of Houston. This work was performed under National Science Foundation Grant ENG-77-14851.

NOTATION

A = dimensionless parameter, Equation (A7)
$\underline{\underline{A}}$ = matrix of coefficients, Equation (10)
a = probability that a particle-particle collision does not result in agglomeration due to high thermal energy
a_f = fiber radius
$a_k(\theta)$ = functions defined by Equation (12)
a_p = particle radius
$b_k(\theta)$ = functions defined by Equation (13)
C_s = Cunningham slip factor, Equation (21)
$c_k(\theta)$ = functions defined by Equation (14)
D = Brownian diffusion coefficient, Equation (20)
F_{pk} = drag force acting on a particle in the k^{th} layer of a dendrite
f = variable with dimensions of frequency, defined by Equation (84)
I_1, I_o, I_{-1} = coefficients, Equations (69), (70) and (76), (77)
$\underline{i}_r$, $\underline{i}_\theta$ = unit vectors of the cylindrical system of coordinates (r,θ), Figure 1
$\underline{i}_{r'}$, $\underline{i}_{\theta'}$ = unit vectors of the spherical system of coordinates (r',θ') Figures 2 and 3
J_1, J_o, J_{-1} = coefficients, Equations (66) to (68) and (73) to (75)
$j(\theta)$ = particle flux density on the fiber surface, Equation (35)
$j_k^{(s)}(\theta')$ = particle flux density on the surface of a particle in the k^{th} layer of a dendrite due to the s component of flow (s=r, or θ)
K = coefficient that depends on the flow model, Equations (31), (31a) and (31b)
Kn_{eff} = effective Knudsen coeficient, Equation (A9)
$Kn_f = l/a_f$ = fiber Knudsen coefficient
$Kn_p = l/a_p$ = particle Knudsen coefficient
k = Boltzmann's constant; also, index
l = mean free path of gas molecules
$M(\theta)$ = integer function of θ defined by Equation (11)
m_k = expected number of particles in the k^{th} layer of a dendrite
$\dot{m}_k = \left(\frac{\partial m_k}{\partial t}\right)_\theta$
m_p = particle mass
$\underline{m}$ = vector having m_k as elements
$\underline{m}_o$ = $\underline{m}$ at birth (t=0)
$N(\tau,\theta)$ = dendrite number distribution function per unit length of fiber, taking into account both sides (upper and lower) of the fiber
$N_o(\tau,\theta)$ = $N(\tau,\theta)$, omitting the shadow effect
$n(r,\theta)$ = particle number concentration around the fiber
n_o = approach particle number concentration for fiber
n_{ok} = approach particle number concentration for a target particle in the k^{th} layer of a dendrite
$n_k^{(r)}, n_k^{(\theta)}$ = particle number concentration around a target particle in the k^{th} layer of a dendrite for the radial and tangential problem, respectively
P = pressure
Pe_f = fiber Péclet number, Equation (44)
$Pe_{pk}^{(s)}$ = particle Péclet number for the k^{th} dendrite layer and the s component of flow (s=r, or θ), Equations (45) and (46)
$R = a_p/a_f$ = interception parameter
$Re_f = 2a_f U\rho_g/\mu$ = fiber Reynolds number
$R_{i,k}^{(s)}$ = rate of increase of m_k by deposition on particles occupying the i^{th} layer due to the flow component in the s direction (s=r, or θ)
r = radial cylindrical coordinate, Figure 1
r' = radial spherical coordinate, Figures 2 and 3
S_p = coefficient defined by Equation (57)
$St_{pk}^{(s)}$ = Stokes number for particle-particle system for the k^{th} dendrite layer and the s component of flow (s=r, or θ)
T = absolute temperature
t = dendrite age
$U = U_s/(1-\gamma)$ = velocity of approach to fiber; also, mean interstitial velocity through the filter
U_s = superficial velocity through the filter
$U_k^{(s)}$ = velocity of approach to particle in the k^{th} layer due to the s component of flow (s=r, or θ)
$\underline{u}_1, \ldots \underline{u}_M$ = eigenvectors of $\underline{\underline{A}}$
v_r, v_θ = radial and tangential flow components around the fiber
$\underline{y}_1^T, \ldots, \underline{y}_M^T$ = eigenrows of $\underline{\underline{A}}$
z = Cartesian coordinate in the main direction of flow

Greek Letters

α = rate of particles approaching a clean fiber per unit length, Equation (8)
β = slip factor, Equation (58)
γ = packing density of filter
ϵ = small positive number (≤ 0.5), Equation (11)
η_o = single clean fiber collection efficiency
θ = angular cylindrical coordinate measured from the downstream stagnation point, Figure 1
θ' = angular spherical coordinate measured from the forward stagnation point, Figures 2 and 3
κ = fraction of gas molecules undergoing diffuse reflection at a surface; $(1-\kappa)$ is the fraction undergoing specular reflection
λ = filter coefficient
λ_o = clean filter coefficient
$\lambda_1, \ldots, \lambda_M$ = eigenvalues of $\underline{\underline{A}}$
μ = gas dynamic viscosity
$\nu_o(\theta)$ = function of θ defined by Equation (80)
ρ = coordination number, that is, maximum number of particles in the $(k+1)$st layer which can be attached directly to the same particle of the k^{th} layer
ρ_g = gas density
ρ_p = particle density
σ = specific deposit (volume fraction of deposited matter)
τ = time measured from the beginning of aerosol flow through the filter
τ_f = duration of filtration run
τ_r = particle relaxation time, Equation (A8)
τ_{ug} = duration of period of unhindered dendrite growth, Equation (86)
$\Phi_k^{(r)}, \Phi_k^{(\theta)}$ = functions defined by Equations (42) and (43), respectively
$\phi_{k,i}^{(s)}$ = fraction of α colliding with a target particle in the k^{th} layer to become part of the i^{th} layer owing to the s component of flow (s=r, or θ)
X_k = constants, Equation (49)
$\chi(t;\tau,\theta)$ = dendrite age distribution function at time τ and angular position θ
Ψ_k = function defined by Equation (65)

ψ = streamfunction of flow around a fiber; also dummy variable

LITERATURE CITED

Astakhov, A. V., "Rate of Brownian Coagulation of Aerosols by the Thirteen-Moment Approximation," (in Russian), *Dokl. Akad. Nauk SSSR*, **161**, 1114 (1965)

Beizaie, M., C. S. Wang and Chi Tien, "A New Theory of Particle Deposition on Single Collectors," (in preparation) (1980).

Bhutra, S., and A. C. Payatakes, "Experimental Investigation of Dendritic Deposition of Aerosol Particles," *J. Aerosol Sci.*, **10** 445 (1979).

Billings, C. E., "Effect of Particle Accumulation in Aerosol Filtration," PhD dissertation, Calif. Inst. Technol., Pasadena, (1966).

Dahneke, B., "Kinetic Theory of the Escape of Particles from Surfaces," *J. Colloid Interface Sci.*, **50**, 89 (1975).

Epstein, P. S., "On the Resistance Experienced by Spheres in their Motion through Gases," *Phys. Rev.*, **21**, 217 (1923).

Fuchs, N. A., *The Mechanics of Aerosols*, pp. 25-29, Pergamon Press, Oxford, England (1964).

Grad, H., "On the Kinetic Theory of Rarefield Gases," *Comm. Pure Appl. Math*, **2**, 331 (1949).

Gradoń, L., and A. C. Payatakes, "Convective Diffusion to a Sphere at Intermediate and Large Knudsen Numbers," (in preparation) (1980).

Happel, J., "Viscous Flow Relative to Arrays of Cylinders," *AIChE J.*, **5**, 174 (1959).

Kanaoka, C., H. Emi and T. Myojo, "Simulation of Deposition and Growth of Airborne Particles on a Filter," (in Japanese), *Chem. Eng. Ponbunshu*, **5**, 535 (1978).

Kirsh, A. A., and J. B. Stechkina, "The Theory of Aerosol Filtration with Fibrous Filters," in *Fundamentals of Aerosol Science*," D. T. Shaw, ed., Chapt-4, Wiley, New York, (1978).

Kuwabara, S., "The Forces Experienced by Randomly Distributed Parallel Circular Cylinders or Spheres in a Viscous Flow at Small Reynolds Numbers," *J. Phys. Soc. Japan*, **14**, 527 (1959).

Lamb, H., *Hydrodynamics*, Dover, New York, (1945).

Levich, V., *Physicochemical Hydrodynamics*, Prentice-Hall, Englewood Cliffs, N.J. (1962).

Natanson, G. L., "Diffusional Deposition of Aerosols on a Cylinder for Small Interception Coefficient," (in Russian), *Dokl. Akad. Nauk SSSR*, **112**, 100 (1957).

Payatakes, A. C., "Model of Aerosol Particle Deposition in Fibrous Media with Dendrite-Like Pattern. Application to Pure Interception During Period of Unhindered Growth," *Filtration and Separation*, **13**, 602 (1976*a*).

Payatakes, A. C., " Model of the Dynamic Behavior of a Fibrous Filter. Application to Case of Pure Interception During Period of Unhindered Growth," *Powder Technol.*, **14**, 267 (1976*b*).

Payatakes, A. C., "Model of Transient Aerosol Particle Deposition in Fibrous Media with Dendritic Pattern," *AIChE J.*, **23**, 192 (1977).

Payatakes, A. C., and L. Gradoń, "Dendritic Deposition of Aerosol Particles in Fibrous Media by Inertial Impaction and Interception," *Chem. Eng. Sci.*, **35** (1980).

Payatakes, A. C., and Chi Tien, "Particle Deposition in Fibrous Media with Dendrite-Like Pattern. A Preliminary Model," *J. Aerosol Sci.*, **7**, 85 (1976).

Sitarski, M., and J. H. Seinfled, "Brownian Coagulation in the Transition Regime," *J. Colloid Interface Sci.*, **61**, 261 (1977).

Tien, Chi, C. S. Wang and D. T. Barot, "Chainlike Formation of Particle Deposits in Fluid-Particle Separation," *Science*, **196**, 983 (1977).

Wang, C. S., M. Beizaie and Chi Tien, "Deposition of Solid Particles on a Collector: Formulation of a New Theory," *AIChE J.*, **23**, 879 (1977).

APPENDIX

Summary of Expressions for Particle Concentration Fields and Flux Densities in the Case of Convective Brownian Diffusion to a Sphere at Low Reynolds Numbers

Consider a particle of radius a_p immersed in an unbounded aerosol flow with approach velocity U_k. Assume, further, that the aerosol particles are monosized with radius (also) a_p and that the bulk number concentration is n_{ok}. At low Reynolds numbers, we obtain the following expressions for the concentration n_k and the flux density on the wall j_k.

Nonslip flow ($Kn_p < \sim 10^{-2}$)

$$\frac{n_k(r',\theta')}{n_{ok}} = 0.870 \int_0^w \exp\left(-\frac{4}{9}z^3\right)dz \tag{A1}$$

with

$$w = \left(\frac{3}{8}\right)^{1/3}\left(\frac{2a_pU_k}{D}\right)^{1/3}\left(\frac{r'}{a_p}-2\right)\frac{\sin\theta'}{\left(\theta'-\frac{1}{2}\sin 2\theta'\right)^{1/3}} \tag{A1a}$$

$$j_k(\theta') = -D\frac{\partial n_k}{\partial r'}\Big)_{r'=2a_p}$$

$$= -0.627\left(\frac{n_{ok}D}{a_p}\right)\left(\frac{2a_pU_k}{D}\right)^{1/3}\frac{\sin\theta'}{\left(\theta'-\frac{1}{2}\sin 2\theta'\right)^{1/3}} \tag{A2}$$

This is the Levich solution, modified to take in account the finite size of adsorbing particles. The angular coordinate θ' is measured from the forward stagnation point.

Slip flow ($\sim 10^{-2} < Kn_p < \sim 1$)

Modifying the results of Gradon and Payatakes (1980) to account for the finite size of adsorbing particles, we obtain

$$\frac{n_k(r',\theta')}{n_{ok}} = 0.870 \int_0^w \exp\left(-\frac{4}{9}z^3\right)dz \tag{A3}$$

with

$$w = \left(\frac{3}{8}\right)^{1/3}\left(\frac{2a_pU_k}{D}S_p\right)^{1/3}\left(\frac{r'}{a_p}-2\right)\frac{\sin\theta'}{\left(\theta'-\frac{1}{2}\sin 2\theta'\right)^{1/3}} \tag{A3a}$$

where

$$S_p = \frac{a_p+2\beta}{a_p+3\beta} \tag{A4}$$

Here, β is the slip factor [see Fuchs, 1964; also, Equation (58)]. The flux density on the wall is given by

$$j_k(\theta') = -D\frac{\partial n_k}{\partial r'}\Big)_{r'=2a_p}$$

$$= -0.627\left(\frac{n_{ok}D}{a_p}\right)\left(\frac{2a_pU_k}{D}S_p\right)^{1/3}\frac{\sin\theta'}{\left(\theta'-\frac{1}{2}\sin 2\theta'\right)^{1/3}} \tag{A5}$$

Free molecular flow ($\sim 1 < Kn_p$)

This problem was solved (retaining the effect of drift) by Gradoń and Payatakes (1980), using the method developed by Grad (1949). Taking in account the finite size of adsorbing particles, we get

$$\frac{n_k(r',\theta')}{n_{ok}} = 1 - A\left[\frac{4a_p^2 - 4a_pU_k\tau_r\cos\theta'}{r'^2 - 2r'U_k\tau_r\cos\theta'}\right]^{1/2} \tag{A6}$$

with

$$A = \frac{17(1-a)^2Kn_{\text{eff}} + 25(1-a^2)}{\frac{3}{2}\pi(1-a^2)Kn_{eff}^2 + [17(1-a)^2 + \frac{5}{2}\pi(1+a)^2]Kn_{eff} + 25(1-a^2)} \tag{A7}$$

Here, τ_r is the relaxation time, given by

$$\tau_r = \frac{2a_p^2\rho_p}{9\mu}C_s \tag{A8}$$

Kn_{eff} is an effective Knudsen number, defined by

$$Kn_{eff} = \frac{2\tau_r}{a_p\sqrt{2\pi m_p/kT}} = \left(\frac{2a_p\rho_p kT}{27\pi^2\mu^2}\right)^{1/2} C_s/a_p \qquad \text{(A9)}$$

and a is the probability that a particle-particle collision does not result in agglomeration. The probability a may be quite significant for very small particles possessing sufficient thermal energy to escape the attractive London-van der Walls force (Dahneke, 1976). Here we assume that the particles are sufficiently large for a to be nil.

The flux density on the wall is given by

$$j_k(\theta') = -D\left(\frac{\partial n_k}{\partial r'}\right)_{r'=2a_p} = -\frac{Dn_{ok}A}{2a_p}\frac{\left(1-\frac{1}{2}St_{pk}\cos\theta'\right)}{(1-St_{pk}\cos\theta')} \qquad \text{(A10)}$$

where St_{pk} is defined as

$$St_{pk} = \frac{2a_pU_k\rho_p}{9\mu}C_s \qquad \text{(A11)}$$

Manuscript received June 28, 1979; revision received December 11, and accepted December 21, 1979.

Forced Convective Boiling in Vertical Tubes for Saturated Pure Components and Binary Mixtures

DOUGLAS L. BENNETT

Chief Engineers Office
Air Products and Chemicals, Inc.
Allentown, Pennsylvania 18105

and

JOHN C. CHEN

Institute of Thermo-Fluid Engineering and Science
Lehigh University
Bethlehem, Pennsylvania 18015

Over 1 000 sets of data for forced convective boiling of distilled water, ethylene glycol and aqueous mixtures of ethylene glycol are reported. Most of these data were taken in the annular flow regime. These data indicate a previously unrecognized Prandtl number effect on the boiling heat transfer for both pure components and mixtures. A significant reduction in the heat transfer coefficient is observed for mixtures attributable to mass transfer effects. An expression is developed which accounts for both of these effects and correlates the experimental data to within a mean deviation of 14.9%. This correlation reduces to the standard Chen correlation for pure fluids with Prandtl numbers close to unity.

SCOPE

Internal forced convective boiling of high Prandtl number liquids and mixtures of liquids is commonly encountered in industry. Previous studies in pure component heat transfer have concentrated on lower Prandtl number liquids, especially water. Furthermore, there are essentially no published data or correlations to account for any effects resulting from the forced convective boiling of mixtures. The objectives of this study were to obtain forced convective boiling heat transfer data for a relatively high Prandtl number liquid and for aqueous mixtures, and to develop a correlation based on these data which hopefully is applicable to other pure components and binary mixtures.

CONCLUSIONS AND SIGNIFICANCE

The results from over 1 000 sets of data are reported for forced convective boiling of distilled water, ethylene glycol and aqueous solutions of ethylene glycol. These results are not correlated well by the standard Chen correlation. The deviations are attributed to an unrecognized Prandtl number effect and a significant reduction in the heat transfer coefficient resulting from mixture effects. The proposed correlation retains the two heat transfer mechanisms postulated by Chen. A modified Reynold's analogy is used which accounts for the Prandtl number effect. For mixtures, the heat transfer coefficient associated with the local turbulence induced by bubble nucleation and evaporation is modified by the Florschuetz and Khan expression. For this datum base, the heat transfer associated with the bulk movement of the vapor and liquid dominates. Mixtures effects for this mechanism are correlated by postulating local composition profiles in the liquid, near the evaporating layer. The proposed expressions correlate the data to within a mean error of 15%. For pure components with Prandtl numbers around unity, the proposed correlation reduces to the standard Chen correlation.

The improved predictive capability of this correlation was not obtained from empirically adjusting correlation coefficients but was obtained by extending phenomenological models. Therefore, it is hoped that this correlation may be generally applicable to other systems.

Correspondence should be addressed to: D. C. Bennett, Chief Engineers' Office, Air Products and Chemicals Inc., Allentown, Pennsylvania 18015.

0001-1541-80-2961-0454-$01.15.